Plasma Chem Plasma Process (2007) 27:349–358
DOI 10.1007/s11090-007-9093-z

ORIGINAL PAPER

MgO Erosion Profile in the High Pressure Coplanar Discharge

Seung Min Lee · Sung Soo Yang · Young Sik Seo · Jae Koo Lee

Published online: 26 July 2007

Abstract The sputtering of the MgO protective layer by energetic ions is one of the factors limiting the lifetime of the plasma display panels (PDPs). The sputtering profile of the MgO layer in a coplanar PDP cell has been studied using two-dimensional particle-in-cell Monte-Carlo Collision (PIC–MCC) simulations. The sputtering profile of the MgO layer for various gas conditions is obtained accounting for the energy and angle distributions of different ion species and their respective sputtering yields. Based on the simulation results, the MgO layer is more aggressively sputtered in Ne-based discharges than in He-based discharges. As a result, it is expected that the addition of He to the Ne-Xe mixture in PDPs will reduce the sputtering of the MgO layer and extend the lifetime of the PDP cells.

Keywords Plasma display panel · Energy and angle distributions · MgO · Erosion

Introduction

Plasma display panel (PDP) is one of the most promising flat panel technologies [1]. However, low luminous efficiency and lifetime have to improve to compete with other display technologies such as liquid crystal displays (LCD) and organic light emitting diodes (OLED). A magnesium oxide (MgO) protective layer plays important roles in PDP cells. Besides protecting the dielectric layer, it provides a large secondary electron

S. M. Lee · Y. S. Seo · J. K. Lee (✉)
Electronic and Electrical Engineering Department, Pohang University of Science and Technology, Pohang, Gyungbuk 790-784, Korea
e-mail: jkl@postech.ac.kr

S. S. Yang
PDP Research Lab. PDP Division, 184 Gongdan-dong, Gumi, Gyungbuk, 730-030, Korea

emission. The sputtering of this layer by ions and fast neutrals causes the degradation of the cell and limits the lifetime of the PDPs. Therefore, it is necessary to find an optimum gas composition for which the damage can be minimized.

When considering only the number of incident ions on the MgO surface, one would expect that MgO sputtering due to Xe ions increases with the Xe concentration. Considering the energy distributions of incident ions on the MgO layer, however, it is difficult to estimate exactly the MgO sputtering. For example, the number of energetic Xe ions decreases with increasing Xe concentrations [2, 3]. There have been several articles estimating the sputtering rate and lifetime of PDPs [4–7]. Most papers, however, are limited to Ne–Xe gas mixtures and do not provide the sputtering profile as a function of the cathode position. Sung et al. [4] reported the calculated erosion distribution in the MgO surface by using 2-D PIC simulations. However, they investigated the erosion calculations assuming the erosion mainly depends on the energy of incidence y-direction to MgO surface. One experiment reported that the MgO erosion by energetic ion bombardments occurs mainly in the inner portion of the cathode region in PDP cells [5]. Although Piscitelli et al. [6] calculated the erosion rate by using hybrid simulation method, they did not calculate ion energy distributions with low energy value and assumed that the sputtering yield of Ne on MgO is the same as that of Xe. Yoon et al. [7] also estimated the sputtering rate and lifetime in the similar condition of PDP cell. However, they could not give the sputtering profile as a function of the cathode position. Although there have been several articles about energy distribution of incident ions hitting the cathode surface [6–9], almost no report mentioned the incident angle distributions of ions on the cathode surface [10, 11]. Considering the peak value of the sputtering yield has the incident angle range of 45–60° [12], the angle distributions of incident ions are necessary to understand the MgO erosion profile.

In this study, we have measured the incident ion energy and angle distributions on the MgO surface in the cathode region for a coplanar PDP cell. We used a 2-D object oriented particle in cell (OOPIC) code [13] and studied discharges at different gas composition (Ne–Xe and He–Xe mixtures). The sputtering yield as a function of the energy and angle of incident ions was obtained using TRIM.[1] Based on the ion fluxes and the sputtering yield, the MgO erosion profile can be estimated. In section "Simulation Conditions", the simulation model and the discharge conditions are presented. The simulation results for the MgO erosion profile in various gas conditions and gas compositions are discussed in section "Results and Discussion". Finally, we summarize our work in section "Conclusions".

Simulation Conditions

Figure 1 shows the two-dimensional simulation domain of a conventional coplanar-type PDP cell. The PDP cell used for the study is 1,080 μm wide and has a height of 210 μm. The gap distance d between the two sustain electrodes is 80 μm and the length l of each sustain electrode is 310 μm. The thickness of the dielectric layers is 40 μm and the dielectric properties include those of the MgO protecting layer. Their relative dielectric constant is 12. To obtain the sputtering profile, we divided the cathode region into fifteen equal parts, as shown in Fig. 1. We have investigated the energy and angle distributions of ions impinging on the MgO surface in the cathode region of this PDP cell. Ne–Xe mixture

[1] http://www.srim.org

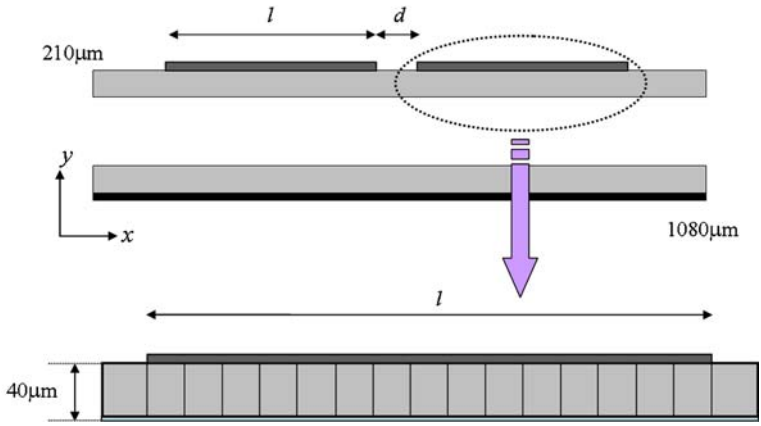

Fig. 1 Two-dimensional PIC-MCC simulation domain of a conventional coplanar-type PDP cell

and He–Xe mixture with 5 and 10% content of Xe at a pressure of 300 Torr have been simulated. The time step Δt and the number of spatial grids in the x and y direction are 5×10^{-13} s, 108 and 84, respectively. The electron density at the beginning of the simulation is 10^{17} m^{-3} and the ion densities are determined using the neutral gas mixture ratio. The number of physical particles per computer superparticle is 5×10^5. The discharge is ignited by applying a 2 μs—300 V pulse between the sustain electrodes. The rising and falling time of the pulse are 0.05 and 0.25 μs respectively. The address electrode was not used in this study and remained biased to half the applied voltage, i.e. 150 V. The constant secondary electron emission coefficients γ_{se} used in the simulation are 0.3, 0.5 and 0.05 for Ne, He and Xe ions, respectively. We also considered elastic, excitation and ionization collisions between electrons and neutrals[2] as well as elastic and resonant charge exchange collisions between ions and neutrals [14, 15]. Ion-neutral charge exchange collisions play a key role in determining the energy distribution of ions in the cathode region. The data presented is obtained by integrating over one pulse of the discharge.

Results and Discussions

Sputtering Yield

To calculate the MgO sputtering profile by He, Ne and Xe ions, we should consider not only the energy and angle distributions of impinging ions but also their respective sputtering yields. The sputtering yields [16, 17] were obtained using TRIM assuming a surface binding energy at 10 eV [7]. TRIM provides the sputtering yield as a function of angle and energy of incident ions. The sputtering yield is obtained by averaging over $\sim 10^5$ incident ions and the incident energy and angle are varied in intervals of 10–20 eV and 5° intervals respectively. Figure 2 shows the sputtering yield by He, Ne and Xe ions impinging on a MgO layer. The sputtering threshold energies are 26 eV for Ne and 44 eV for He irrespective of the incident angle of ions. In the case of Xe ions, however, the sputtering

[2] The Siglo Database, Kinema Research & Software, http://www.kinema.com/

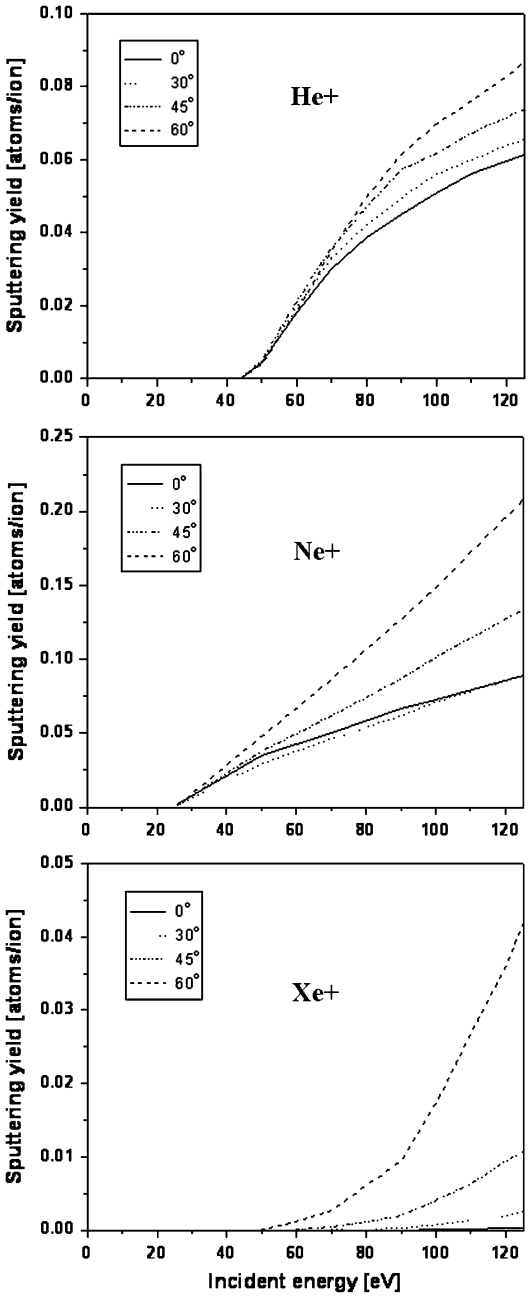

Fig. 2 Sputtering yield for He, Ne and Xe ions as a function of energy and angle of incidence. Results obtained using TRIM

threshold energy reduces gradually as the incidence angle of the Xe ions increases [18]. We also found that the sputtering yield of Ne ions is larger than that of He and Xe ions because the mass of Ne ions is comparable to the mass of Mg and O atoms. Therefore, despite the low Ne ion concentration in the discharge, it is expected that Ne ions contribute significantly to the sputtering of the MgO layer due to their low sputtering threshold energy

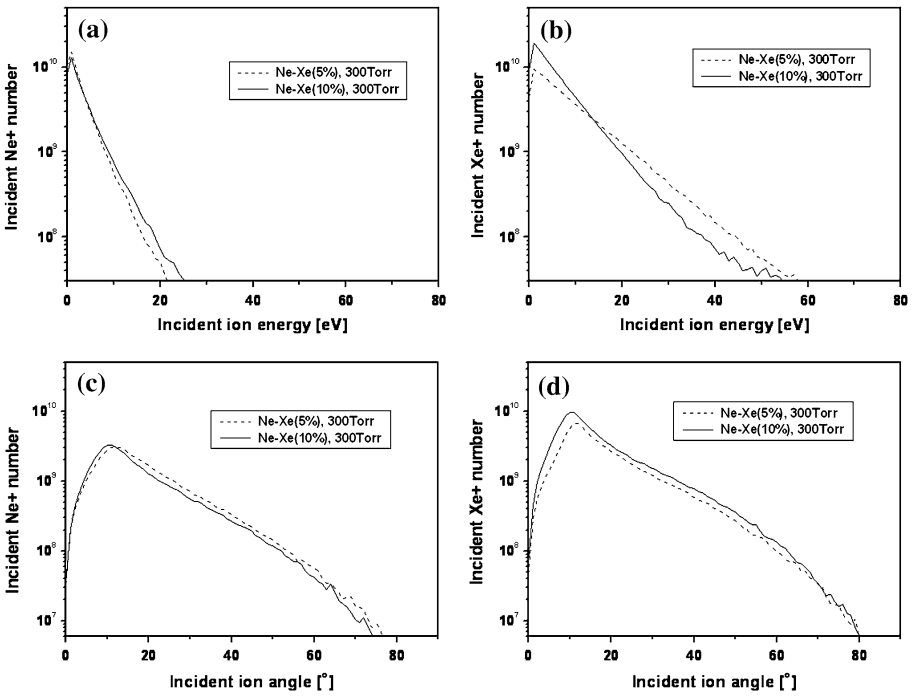

Fig. 3 Energy and angle distributions on the dielectric surface in the cathode region as a function of Xe content in Ne–Xe discharges at 300 Torr; (**a**) Ne ion energy distribution, (**b**) Xe ion energy distribution, (**c**) Ne ion angle distribution, (**d**) Xe ion angle distribution

and their high sputtering yield. Although the sputtering threshold energy for Xe ions is slightly larger than that for He ions in the He–Xe mixture, Xe ions are more abundant and control the sputtering process.

Energy and Angle Distributions of Incident Ions

The energy and angle distributions of incident ions on the MgO layer in the cathode region of a coplanar-type PDP cell are plotted in Fig. 3 for a Ne–Xe discharge at 300 Torr. Despite the low concentration of Xe gas in the Ne–Xe mixture, Xe ions are more abundant than Ne ions due to their lower ionization energy and larger ionization cross section. Charge exchange collision in the cathode sheath region plays an important role in determining the energy distribution of impinging ions on MgO surface. Given the low percentage of Xe (5%), Ne neutrals are more abundant than Xe neutrals and Ne ions are more likely to undergo resonant charge exchange collisions than Xe ions. As a result, Ne ions are less energetic than Xe ions. However, when the Xe concentration is increased from 5 to 10%, the energy distributions of Ne and Xe ions show opposite trends. The high energy tail of the Xe ion distribution decreases while that of the Ne ions increases, as shown in Fig. 3a, b. The reported energy distribution of incident ions on the cathode region from hybrid simulations is also consistent with our simulation results [6, 8]. Based on our simulation results, we can expect that the contribution of energetic Ne ions to the sputtering of MgO

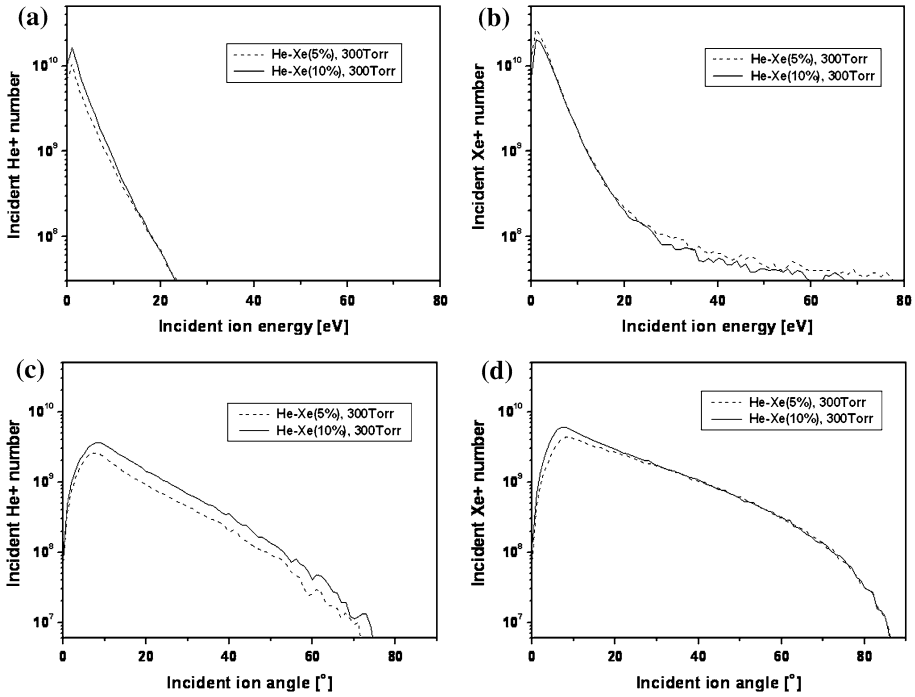

Fig. 4 Energy and angle distributions on the dielectric surface in the cathode region as a function of Xe content in He–Xe discharges at 300 Torr; (**a**) He ion energy distribution, (**b**) Xe ion energy distribution, (**c**) He ion angle distribution, (**d**) Xe ion angle distribution

protecting layer will be larger as the Xe partial pressure is increased. For the He–Xe mixture, we have obtained similar trends. The number of He ions, however, is smaller due to its higher ionization energy (Fig. 4a, b).

Figure 3c, d show the incident angle distributions of Ne and Xe ions on the MgO layer of the cathode region. Most Ne and Xe ions impinging on the dielectric surface have incident angles below 40° with a peak around 12°. This contrasts with the angle distributions in a matrix-type PDP cell, where the angles are smaller with a peak around 3° [10, 11]. The angle distribution of Ne ions is slightly reduced and that of Xe ion increases as the Xe concentration increases. The angle distribution of Xe ions is also broader than that of Ne ions. The incident ion angle distributions in the He–Xe mixture are similar to the Ne–Xe case. The angle distribution of Xe ions in the He–Xe mixture, however, is broader than that of Xe ions in the Ne–Xe mixture, as shown in Figs. 3d and 4d. This means that the MgO sputtering due to Xe ions is larger in He–Xe mixtures. Using the energy and angle distributions of incident ions in each of the fifteen divisions of the cathode, the sputtering profile of the MgO layer can be estimated.

MgO Erosion Profile

In order to obtain the MgO sputtering profile, we combined the energy and angle distributions of impinging ions from two-dimensional PIC–MCC simulations with the sputtering

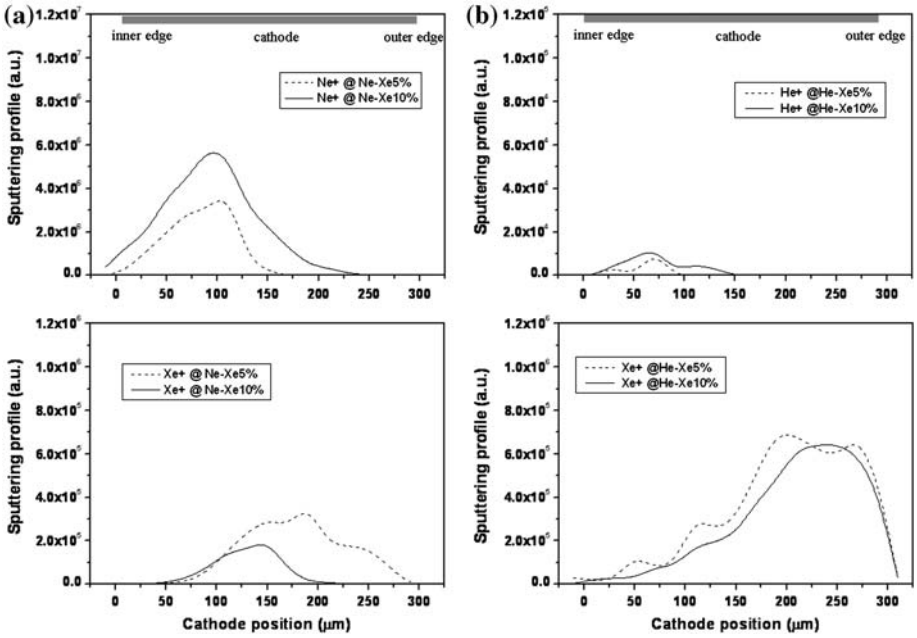

Fig. 5 Sputtering profiles due to (**a**) Ne and Xe ions in Ne–Xe mixtures and (**b**) He and Xe ions in He–Xe mixture obtained using 2-D PIC–MCC and TRIM simulation data

yield of ions (Fig. 2). Figure 5a, b show the sputtering profile for two Xe concentrations in Ne–Xe and He–Xe mixtures. The increase of Xe content increases the erosion of the MgO layer due to the increase of high energetic Ne and He ions (Figs. 3a and 4a). He ions, however, have little effect on the MgO erosion when compared with Ne ions. Although the erosion caused by the buffer gases (Ne or He) occurs in regions closer to the inner portion of the cathode [5], that by Xe ions occurs rather in the outer portion of the cathode. This different behavior is a result of the spatio-temporal evolution of the potential profile, the different ion inertia and the strong angle dependence of the sputtering yield of Xe ions.

Figure 6 shows the energy (eV) and angle (radian) distributions in the fourth and last parts of cathode region for a 300 Torr discharge with a 5% of Xe. Although a large number of Ne ions exceed the sputtering threshold energy (26 eV) in the fourth region (Fig. 6a), there are no Ne ions with energies above the sputtering threshold energy in the last region (Fig. 6b). This results in the sputtering profile, as shown in Fig. 5a.

Figure 6c, d show the energy and angle distributions of Xe ions in a He–Xe discharge. Although the number of Xe ions in the last cathode region is lower than in the fourth region, there are many Xe ions with a high incidence angle. Since the sputtering yield increases and the sputtering threshold energy also decreases with the incidence angle (Fig. 2), the MgO sputtering profile by Xe ions is shifted to the outer edge of the cathode.

The influence of He and Ne ions on the MgO erosion is compared in Fig. 7a for a fixed Xe concentration (5%). The MgO sputtering by Ne ions is the highest because of their low sputtering threshold energy and their high sputtering yield. Although we magnified the sputtering profile by He ions 10 times, the sputtering due to He ions is negligible. The MgO sputtering by Xe ions is smaller than that by Ne ions (Fig. 7b). Based on our simulation results, the addition of He to the gas mixture used in PDPs (typically, Ne–Xe mixtures) is

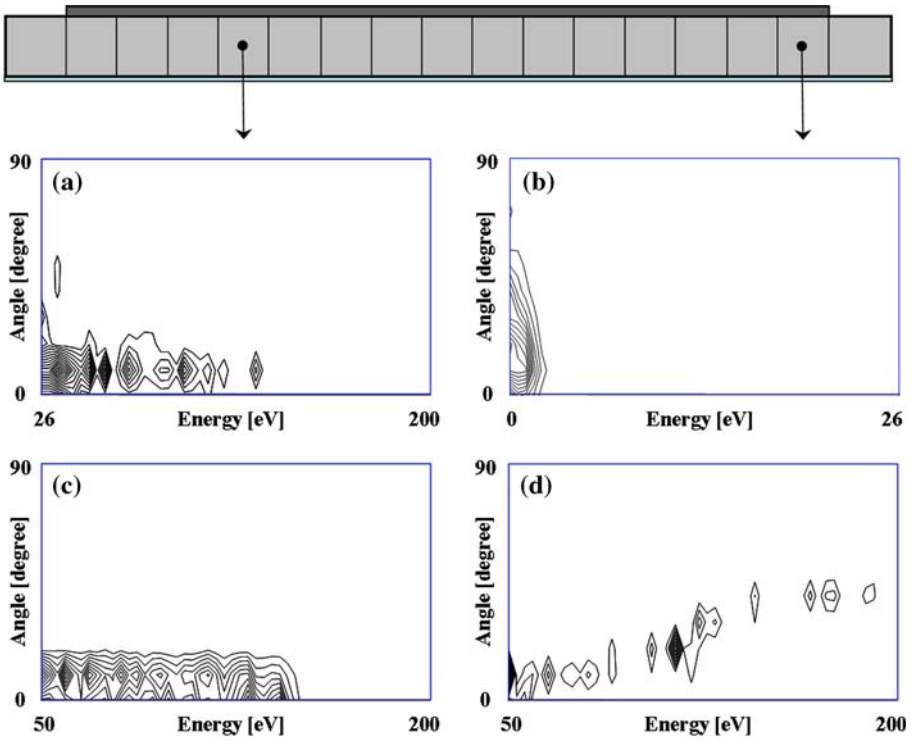

Fig. 6 Energy and angle distribution of Ne ions in a Ne–Xe mixture in the (**a**) fourth and (**b**) last division of the cathode region. Energy and angle distribution of Xe ions in a He–Xe mixture in the (**c**) fourth and (**d**) last division of the cathode region

expected to reduce the sputtering of the MgO thin layer, extending the lifetime of the PDP cells. Since our simulation results are only the estimation on MgO erosion profile by ions obtained during the first pulse of the discharge, it may be different from experimental results. For better comparison with experiments, the energy and angle distribution should be obtained for discharges that include the residual surface charge from previous pulses.

Conclusions

The MgO sputtering profiles for various gas conditions have been estimated by combining the energy and angle distributions of impinging ions from two-dimensional PIC–MCC simulations with the sputtering yield obtained using the TRIM. As the Xe concentration increases, the number of energetic Ne and He ions increases and He and Ne ions contribute significantly to the sputtering of the MgO thin layer. On the other hand, the sputtering due to Xe is reduced. The contribution of He ions to the MgO sputtering is much smaller than that of Ne ions. Therefore, in addition to improving the brightness and luminous efficiency [19], the addition of He to the gas mixture is expected to reduce the sputtering of the MgO thin layer and extend the lifetime of the PDP cells.

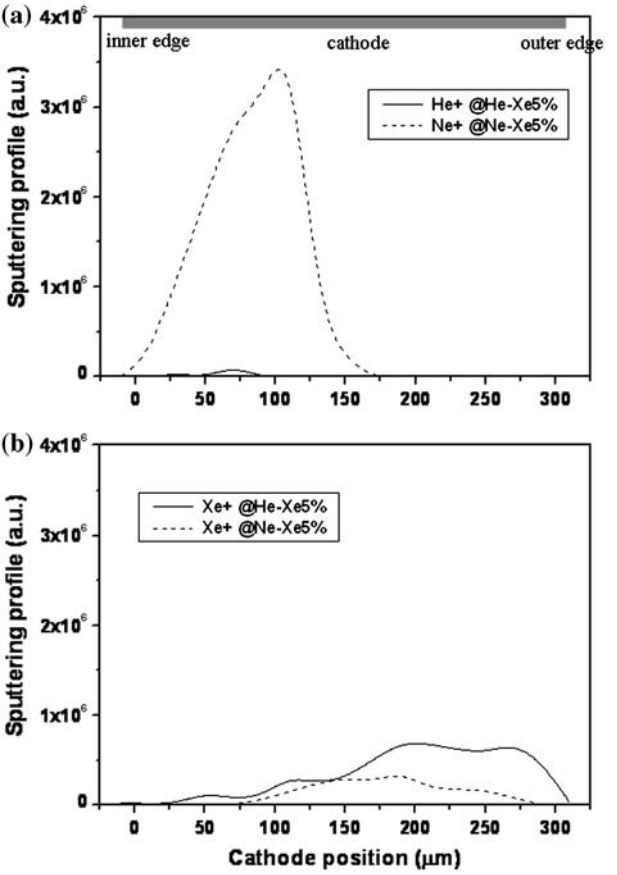

Fig. 7 Comparison of the MgO erosion profile in Ne–Xe and He–Xe mixtures with same Xe concentration (5%). Erosion caused by (**a**) Ne and He ions (**b**) Xe ions

Acknowledgements This work was supported by LG Electronics, LG Micron and Korea Science and Engineering Foundation (KOSEF) grant funded by the Korea government (MOST) (No. R01-2007-000-10730-0).

References

1. Lee JK, Verboncoeur JP (2001) In: Hippler R et al (ed) Low temperature plasma physics. Wiley-VCH, Berlin, pp 367–385
2. Boeuf JP (2003) J Phys D Appl Phys 36:R53–R79
3. Shin YK, Lee JK, Shon CH, Kim W (1999) Jpn J Appl Phys 38:L174–L177
4. Sung YM, Wada M, Otsubo M, Honda C, Son CH, Kim YK, Park CH (2004) Jpn J Appl Phys 43(2):800–808
5. Choi SH, Shin GY, Lee SI, Oh SG (2000) In: Proceedings of international meeting on information display, pp 487–490
6. Piscitelli D, Callegari Th, Ganter R, Pitchford LC, Boeuf JP (2001) In: Proceedings of the 8th international display workshops, pp 825–828
7. Yoon SJ, Lee IS (2002) J Appl Phys 91(4):2487–2492

8. Piscitelli D, Pitchford LC, Boeuf JP (2000) In: Proceedings of the 7th international display workshops, pp 735–738
9. Hagelaar GJM, Kroesen GMW, Klein MH (2000) J Appl Phys 88(5):2240–2245
10. Yang SS, Kim SJ, Lee JK (2004) J Plasma Fusion Res 82(2):132–136
11. Kim HC, Iza F, Yang SS, Radmilovic-Radjenović M, Lee JK (2005) J Phys D Appl. Phys 38:R283–R301
12. Lieberman MA, Lichtenberg AJ (2005) Principles of plasma discharges and materials processing. John Wiley & Sons, New York, pp 576–579
13. Verboncoeur JP, Langdon AB, Gladd NT (1995) Comput Phys Commun 87:199
14. Raizer YP (1991) Gas discharge physics. Springer-Verlag, Berlin
15. Almeida PGC, Benilov MS, Naidis GV (2002) J Phys D Appl Phys 35:1577–1584
16. Okazawa K, Shidoji E, Makabe T (1999) J Appl Phys 86(6):2984–2989
17. Lu J, Kushner MJ (2000) J Appl Phys 87(10):7198–7207
18. Yamamura Y, Bohdansky J (1985) Vaccum 35(12):561–571
19. Lee HJ et al (2005) In: Proceedings of international meeting on information display, pp 171–174